

Design of an Electromechanical Anthropometric finger and a PID controller for the wrist for applications in Prosthetics

Shreyas Ragavan

Abstract—The design of the finger to be attached to a modular prosthetic hand and a controller solution for the wrist are explored in this effort.. A novel design of a sliding body has been proposed where the outershell, providing form to the finger can be slid in or out off a of a light weight chassis and tightened with a screw. In addition to this the end effector is removabl. This provides an easy method to inspect the mechanism especially as the wiring and the motors are embedded inside.The report deals with key aspects such as the using the forward kinematics (Denavit-Hartenberg equations (DHE)) to component selection for building the model. The wrist is treated as as separate design issue and a Proportional Integral Derivative (PID) controller has been designed and manually tuned to control the rotation of the wrist, using Simulink. Though these continuous equations applied, are assuming ideal conditions, a saturation of the output provides realistic limits and conditions and a more realistic view of what occurs. The results obtained and the tuning process are explained and the conclusions are reached.

Index Terms—, Denavit Hartenberg equations (DHE), Forward Kinematics, Prosthetic hands, PID controller,

I. INTRODUCTION

The objective of this effort is to design a single digit which is a part of a modular prosthetic hand. The aspects of control are explored by implementing a PID controller for the wrist of the prosthetic hand. A prosthesis as a tool makes no pretence of trying to replace the lost limb physiologically but it works as an aid to help provide some of the lost functions and is an interchangeable device worn and used as needed, [4].

The human hand is a multifunctional organ with over 20 degrees of freedom(DOF) and worthy of being emulated by robotic systems, and is complex, [5]. The human finger constitutes of 3 segments or phalanges i.e. the proximal, middle and distal connected by three joints. The progress is mapped in terms of order of the design methodology presented. The wrist controller is dealt with as a separate object and its only relationship to the fingers is the contribution towards weight and inertia. Therefore, the fingers

just form a lumped equivalent mass.

The system is broken down into equations for the torque input which is being given. This equation is the so called ‘plant model’ used in the modeling of the controller. Ideal conditions are used with no accounting for friction and real world conditions. This is acceptable in terms of the complexity involved and lack of computing power. The above is dealt with in section

The advantages of the modern electric prosthetic hand over the traditional version is mainly brought about by the advent in micro controllers, EMG sensors and micro actuators as body power or actuating mechanisms. The superiority is established in terms of weight and capabilities i.e possible positions and orientations of the end effector, i.e DOF’s, with its characteristic adaptability and control techniques.

General Design Intents:

The weight, power consumption, response speed , cost , modularity in design are the different design aspects to be considered in a prosthetic hand,[3],[7],[8]. In most cases, this has been facilitated** by using a strong power with high torque capabilities which facilitates holding objects, though it is quite dependent on the orientation of the fingers towards each other. There are a few hand models that are well known in terms of their capability and thus, good design. .

II. DIGIT DESIGN

A. Description of the design with discussions :

There are totally 4 actuators required in this model to provide the equivalent DOF. Each finger segment has a chassis with grooves on the outer side to enable the body to be slid in/out. The actuators are located in the medial and proximal links of the model with an another actuator at the base joint to provide an additional DOF,adapted from [5] , located near the top provide the additional DOF which can be called ‘wiggling’. This was done to get closer to the kinematics of an actual human finger which can move laterally to a certain degree and the amount of movement was decided at 10° as shown in figure 4

A novel slider and tightening with screw mechanism has been designed as shown in figure 1. The end effector is attached to

the top of the last segment as a detachable and separate unit and thus providing a mechanism through which the sensor can be changed or repaired by simply removing the top which is detachable. The chassis design is simple and hassle free from the point of view of clean and objective design. Further to that, as the chosen DOF for each joint other than the base joint is 1, the design was simplified a great deal. thus be able to spread out.

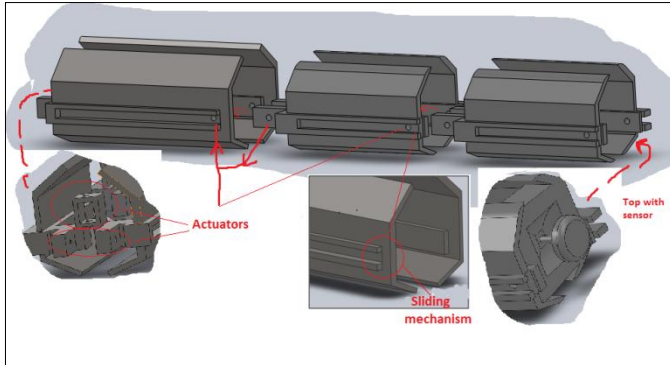


Figure 1 Design and the highlights

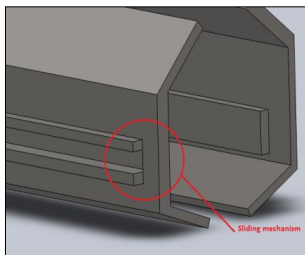


Figure 2 Sliding mechanism highlighted

The weight has been given adequate consideration considering that the grooves reduce mass and still maintain the rigidity required for the finger to be able to withstand some force. It could be made of Carbon fibre to enhance the strength to weight ratio. A firm rubber like covering or possibly lightweight plastic would be mounted on the sides for the body and the shape can be thus varied. The hexagonal shape has been given for additional strength of the structure and also to provide for the various mechanisms highlighted above.

The disadvantages of conventional DC motors with the wiring and paraphernalia has been highlighted in []. Some thought was given in this direction and it is reasoned that a computer program could be written to automate the control of the hand and the microchip could be designed to placed unobtrusively in a belt buckle or wrist watch. The miniaturization that is possible these days would make that a viable solution though this is not explored further in this report.

Considering that a considerable amount of weight has been saved with the structure, an emphasis followed in we can afford to allow a little more weight for the actuators. It was considered that the actuator responsible for lateral motion might require higher torque but since the angle of motion is 10 degrees and for the sake of functionality the motor was chosen to be, geared for lower rotation speed and set for a higher

grasping power, There torque output of the motors are in the range of 78Nm to 217Nm [12].

Approximate Bill of materials:

ITEM	QUANTITY	PRICE, £
Geared DC Motor	4	120
Sensors (As required)	3	30
Position and Current sensors	4	15-30
Microprocessor (depending on type. (8/16/32 bit)	1	20 upwards
Chassis	100gm	20
Wiring	10gm	5
TOTAL PRICE		Approx 225£

III. KINEMATICS

A. Introduction: The forward kinematics method was applied on the proposed digit and the DHE used to calculate the transformation matrix of the finger. The work space is hence calculated from a suitably modified MATLAB program for a 2-jointed robot , [1]. By studying the methods used for the same, the increase in complexity is apparent along with the high computing power requirement, when dealing with higher DOF and complex models. A 4 DOF model was chosen, as an optimum challenge and reasonably closer to the capabilities of a human hand, which is after all the objective of a prosthesis.

A 3 DOF model was also tested in terms of the computation time taken for calculating the workspace. It was approximately half the time taken for the 4 DOF model. The processor used was a dual cored Intel i5 with a turbomax frequency 2.53GHz which is a reasonably up to date configuration. The model is simplified due to the reason that the joint axes are all parallel and the motion is similar. *However*, one simplification was made in the current kinematical analysis, that the distance between the 2 base joints, seen in the 3D model, figure , is zero, as shown inn figure. The distance is negligible compared to the dimensions of the entire finger. A similar kinematic model can be found in [5].

B. Representation in terms of Coordinate Axes : The figure 1, shows the degrees of freedom and over the co ordinate axes chosen at each joint to fascilitate the calculation process. Terminology : The angle of rotation of each joint is depicted by $\Theta_{0,3}$ around the corresponding coordinate axes and frames $(X,Y,Z)_{0,3}$. The axes are decided by the right hand rule. To

perform the kinematics, the simple methodology is to

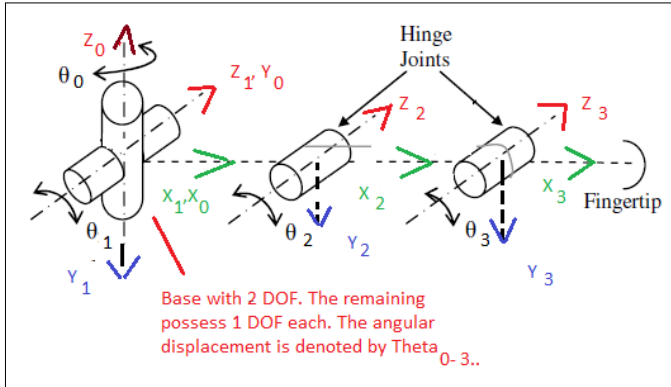


Figure 3 Coordinate Axes and terms adopted

align each coordinate axis of the previous point with the axis of the next point as shown in figure, i.e. One must have the (X,Y,Z)'s pointing in the same direction, and the manipulation required to achieve that is noted down (figure 4). As we progress from the left, the base Coordinate frame 0 (X,Y,Z)₀ must be rotated 90° in the negative direction about the common X axis. to align Z₀ and Z₁ (α_i). After which there is a distance to cover in terms of the Link length. These lengths and allowable rotation have been shown below in figure 4: This is termed as the application of the DHE.

Link	Allowable Rotation about z _i axes (Θ _i) _{i=0-3}	Lengths (along the x _i axes)	Rotation about the x _i axes (α _i)
0	10°	0	-90°
1	80°	28.5mm	0
2	70°	19.3mm	0
3	50°	27.7mm	0

Figure 4 Parameters being defined

C. Applying the DHE :

The above information is input into a homogenous transformation matrix as shown in figure 5, where S and C stand for sine and cosine respectively. The final transformation matrix formed is shown also shown in figure 5.

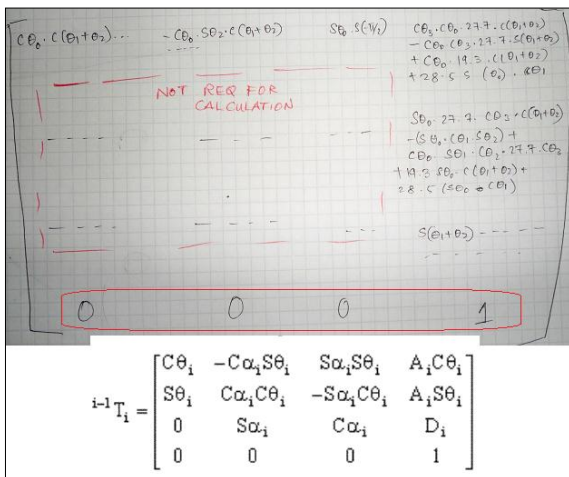


Figure 5 Homogenous Transformation Matrix, [1] shown below and the Final transformation Matrix ⁰T₃

It is natural that one is interested in the area within which the model can function. This is defined as the workplace of the robot.

D. Calculating Workspace of the robot:

The above information, from figure 5 i.e the top two displacement values of the homogenous matrix is input into MATLAB and the code is shown in figure 6 and the resulting workspace is shown in figure :

```
hold;
for A = 0: 0: 0.03 : 0.174
for B = -0.261: 0.03: 1.396
for C = 0: 0.03: 1.221
for D = 0: 0.03: 0.872
plot (cos(D)*cos(A)*27.7*cos(B+C) - cos(A)*cos(D)*27.7*sin(B+C) + cos(A)*19.3*cos(B+C)+28.5*cos(B)*cos(A), ...
sin(A)*27.7*cos(D)*cos(B+C) - (sin(A)*cos(B)*sin(C)+cos(A)*sin(B)*cos(C))*27.7*cos(D) + 19.3*sin(A)*cos(B+C)+28.5*sin(A)')
end
end
end
end
xlabel('Displacement X (m)')
ylabel('Displacement Y (m)')
title('Three link robot arm workspace with angles(theta(i) , 0<i<3) +/- 10,80,70,50 degrees')
```

Figure 6 MATLAB code developed

The movement can be visualized from figure 7 and it seems logically correct within the parameters of movement of a finger. It was attempted to be as close to anthropological movements and it can be seen the fingers can curve slightly backward and angles have been given to facilitate that, which can be seen in the code in figure 5.

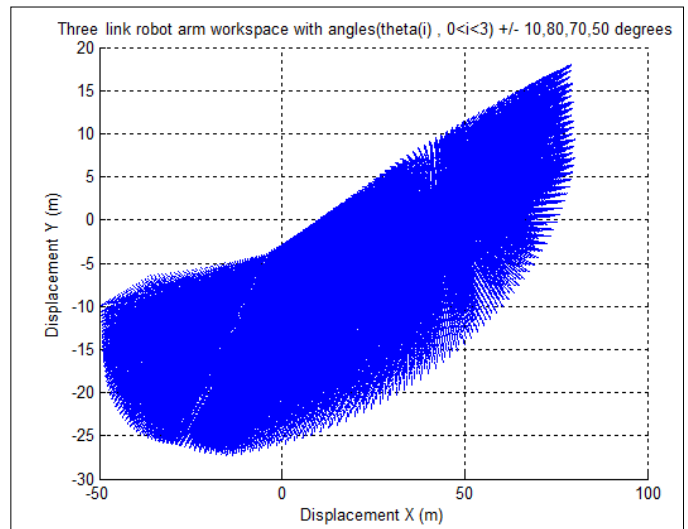


Figure 7 Workspace of the model

IV. PID CONTROLLER FOR THE WRIST

A. Summary of the PID controller:

The PID controller, feeds forward to the plant a proportion of the actuating signal plus its derivative for the purpose of improving the transient response of a closed loop system.[2].

The governing equation of a PID controller can be broken down as:

$$\text{Output} = K_p * \text{Proportional error} - K_d * \text{Derivative error} + K_i * \text{Integral error};$$

The proportional term is an output value based upon the difference between the set point and the actual input value.

The derivative term is based upon the first derivative of the proportional error, or, the velocity of the error. I.e. is the error getting smaller or larger as time goes by.

The integral term is the opposite of the derivative term: it is the sum of all errors over time. The integral term is included to allow the controller to advance the output such that all errors eventually get cancelled, [9]

The constants, K_p , K_d and K_i are factors, commonly known as gain values. The equation is thus weighted. These factors will change based upon the quality of the motors, the weight of the robot and the charge of the batteries driving the motors. A manual trial and error method coupled with hints from [1,9].

B. Design in Simulink and setting up of parameters:

This controller was designed and simulated using Simulink. Figure 8 shows the basic configuration of the control system. The individual components are labelled and function as described above. The two scopes before and after saturation block was put in to highlight the difference in the waveform and effective functioning of the saturator. Notice the ranges of the fluctuations which has been set to a value of +/- 1 Nm as specified in the task. It should be mentioned that with No saturation, i.e. Saturation = 0 , the output is exactly like the input square wave.

It is known that the equations being applied here are meant for ideal conditions and are linear,[1]. Real world conditions and disturbances and unforeseen circumstances, i.e. non linear effects are disregarded in this analysis. It is therefore, possible that the real behaviour be very different from that predicted in the simulation. To approximate for these effects, which are basically, delays related to efficiency and actuator starting characteristics, saturation, or range is set. The square wave is used as the input signal as it offers the possibility of exploring the upwards and downwards transient frequency behaviour. Since sine waves are closely associated with frictional and other non linear characteristics which are not considered here, the square wave is the option chosen..

The precision of the controller can be discerned from the frequency level that it can handle. With this particular saturation level, the level of frequency achieved was quite low, i.e. 0.5 Hz whereas PID controllers are known to be used for frequencies upto 2Hz.

C. System Description and plant model equations:

The scenario given, is that the input of the PID controller is the motor torque, is converted into an angular displacement. The motor torque is approximated by a square wave generator shown at the beginning. It is also taken to the Multiplexer (MUX) so as to get a comparison in the result scope. The PID controller comes next. The Gain function block is used to multiply a factor to the input and the proportional part is

simply performed by the gain block. The integrator and Derivative blocks are used for the I, D parts of the controller. The gains are respectively shown. The outputs are all algebraically added together and routed into the MUX mentioned before

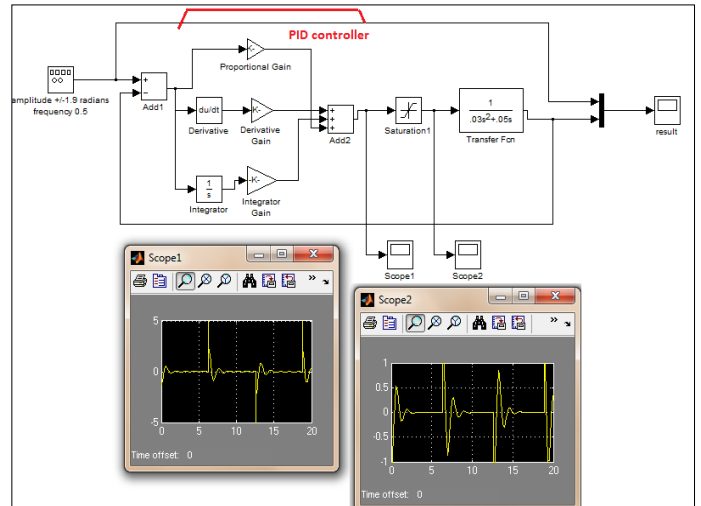


Figure 8 Simulink diagram and Saturation effects

.The constraint of the angle of +/- 110° has been achieved by the logic that if the amplitude of the input, i.e. the required amplitude is never higher than the imposed limit then the control is established. Therefore at the input wave generator, the limit of 1.9 radians, was input into Simulink.

A ‘plant model’ was mentioned in the introduction section. It is created from the transfer function which is nothing but the Laplace transformations of the integrals for easier integration or mathematical operations. Details can be found in [2].

It is clear here that that if we consider the rotational displacement to be Θ , then the torque(T) produced by the motor can be given by the equation :

$$T = I \times \alpha + C \times \omega \dots \dots \dots (1)$$

where I is the moment of inertia and C is the rotational damping (given .03 kg m² and .05 kg m²/s) and α is the angular acceleration and the angular velocity. If we represent the above terms of Θ , angular displacement, then (1) becomes :

$$T = I \times \frac{d^2\theta}{dt^2} + C \times \frac{d\theta}{dt} \dots \dots \dots (2)$$

By applying the transfer function, we get the equation :

$$\text{Displacement is} = \frac{1}{Is^2 + Cs} \dots \dots \dots (3)$$

This is the plant model which is applied in the Simulink circuit shown in figure 8.

D. Tuning the PID controller:

The Ultimate Sensitivity Method was used in finding the gain coefficient values(P, I, D). This method is outlined in [1] .

This involves first setting I and D to 0 and adjusting P to get the desired shape of the graph. From the equations shown in the previous section , it is clear that P induces a large spike in the behaviour of the graph whjich is characterised by the peaks shown in the figure below. It was considered that I and D perform the opposite functions and hence must be close related in terms of what the difference between these values were and the relation to P.

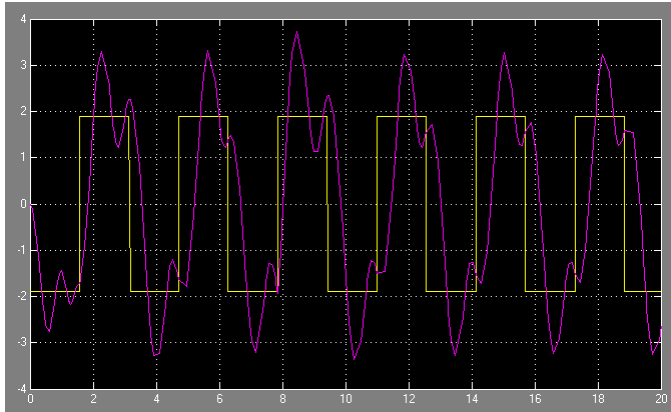


Figure 9 Amplitude of the output Vs Time on the X axis

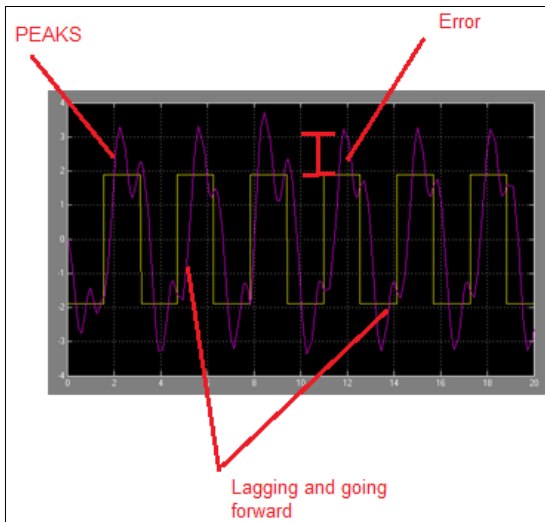


Figure 10 Errors highlighted.

Keeping D and I at 0, it was found that increasing P beyond the value of 15, there was no change in the graph. So this value was kept constant. Now attention was given to the D and I inputs by giving D =0 and I =1. It was found that increasing the integrator values beyond a point say, 7-8, the peak of the graph just went on increasing. And the lowest poeak was attained at 1 and also at values lesser than 1.

There fore , I was set and then D was varied. In this way, after a lot of variations, a final value was arrived at which was that P= 0.7 , I=0.01 and D=0.04. This result is shown in figure 9.

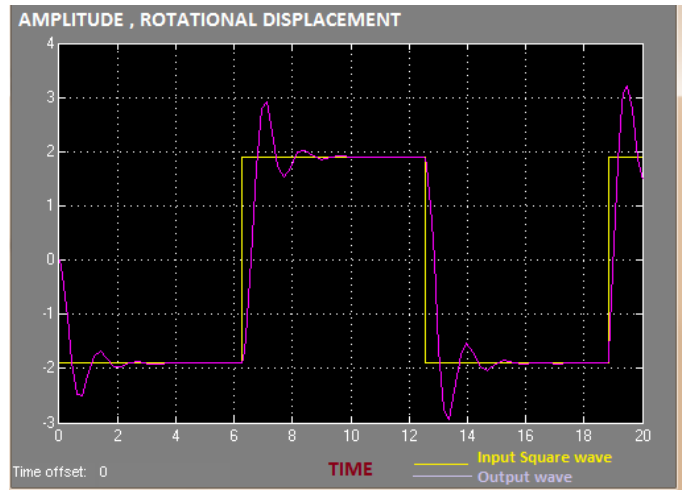


Figure 11 Final Tuned results

The final tuned results are shown in figure 11. The highest peak being formed had the least amplitude at this setting and this seemed to be a threshold below which the results got unpredictable, i.e they varied in amplitude throughout.

However, the errors highlighted in the previous results (figure 10) still remain. Changing the saturation and trying the same results at a higher limit may give more information in this regard. The input frequency amplitude may be increased and this angle may be explored.

Though the above seems clear enough, through the design process, it was found that it is complex indeed to tune a PID controller and probably nearly impossible to exactly match the input in general cases. To get exact results, a great deal of trial and error and intelligent manoeuvring is required for attaining results within a short period of time. It is then, easy to understand why references are made to suitable and unsuitable controllers and it is also clearly seen through [1] that the PID controller is not really suitable for this particular purpose.

However, it should be noted that digital tuners exist , even as inbuilt functions blocks in Simulink. This aspect has not been explored in this report. The characteristics of delay, overshoot and even leading the signal and variation of response over time was pronounced. It is known that the characteristics vary over time,[1].

V. CRITICAL REVIEW AND CONCLUSIONS

The performance of high level technology, albeit, more expensive can be found in [4] , where the designed digit has a hybrid actuation system including a, Shape Memory Alloy (SMA), which retain a memory of the shape and the changes in the length of the alloys result due to voltage changes. However , a wide range of single digit models are similar to the model described here . Infact, miniaturization and use of better materials and higher efficiency have resulted in

electromechanical models which are functional and aesthetic as well. A prosthesis with over 50% weight reduction has been discussed in [7], highlighting the focus on the low weight requirements. The design methodology of this model highlights the efficiency in weight distribution. The chassis structure which runs throughout like a backbone has been modeled on a vehicle and is a proven system. Alternative actuation techniques, is an aspect that is worth exploring. However in terms of functionality this design, including the controller should not be lacking in anyway. Belt type actuators are very suitable for power applications as they transmit braking forces better and can hold positions.

Better controller output is definitely required. The PID controller tuning provided results within a certain range of reasoning. But some effort should go in the direction of the techniques and the behavior of other types of controllers suited to controlling rotary motion could have been explored further.

However, for providing the lateral motion, the torque is applied on the base segment alone. The chassis should be designed such that the base is stronger. In specific, when the lateral motion occurs there will be excessive force on one of the hinges ,where the motor shaft is also attached. This has been neglected for simplicity and assuming that forces will not be high enough to affect the stability. The span of motion is also on the lower side relative to the other spans. The chassis structure is such that, the motor causing lateral motion has its torque distributed as evenly as the rotation in the other direction.

REFERENCES

- [1] Dr.R.C Richardson, "MECH 5090 course lectures."
- [2] Norman.S.Nice, "Control Systems Engineering 4th edition" Wiley- ch 1,2,12
- [3] L.H. Han H.P. Huang, 'Development of A Modular Prosthetic Hand-NTU-Hand III', Department of Mechanical Engineering of Taiwan University
- [4] Beng Guey Lau, "An Intelligent Prosthetic Hand using Hybrid Actuation and Myoelectric Control", The University of Leeds
- [5] Vishalini Bundhoo and Edward J. Park , "Design of an Artificial Muscle Actuated Finger towards Biomimetic Prosthetic Hands", IEEE.
- [6] Rajiv Doshi, BS; Clement Yeh, BS; Maurice LeBlanc, CP, MSME , "The design and development of a gloveless endoskeletal prosthetic hand", Journal of Rehabilitation Research and Development , Vol. 35 No. 4, October 1998, Pages 388-395
- [7] "Shadow Dexterous Hand C6M – Technical specifications manual 2009" , www.shadowrobot.com
- [8] Jeffrey E. Erickson, Graduate Student Member, IEEE, Kathryn J. DeLaurentis, PhD, Mourad Bouzit, PhD, "A Novel Single Digit Manipulator for Prosthetic Hand Applications" , IEEE
- [9] www.societyofrobots.com - PID information -

REFERENCES (FIGURES)

1. Modified from [5] in Paint.